CCR2 inhibition reduces tumor myeloid cells and unmasks a checkpoint inhibitor effect to slow progression of resistant murine gliomas

Supplementary Information:

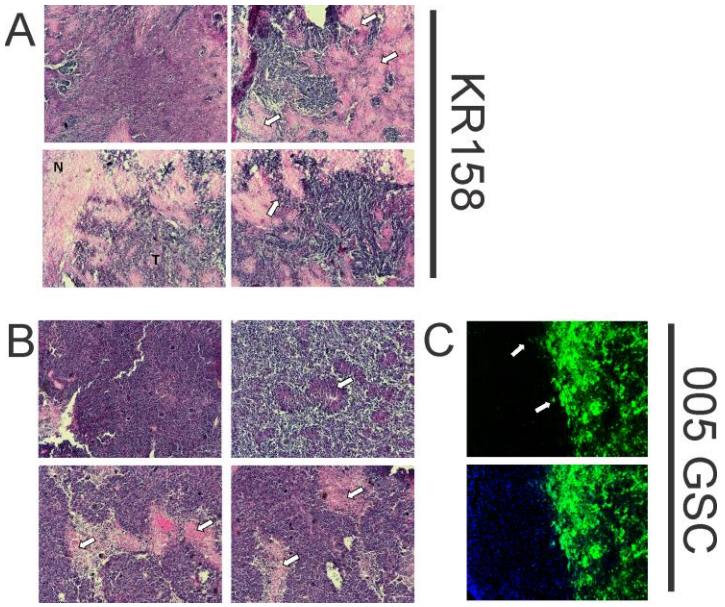

Figure S1: Histological characterization of KR158 and 005 GSC gliomas.

A) Hematoxylin and eosin (H&E) stained images of KR158 gliomas depicting areas of increased cell density (upper left), necrotic regions within the tumor (upper right, white arrows), tumor boundary (T) showing invasion of normal brain parenchyma (N) (lower left), and pseudopalisading necrosis (lower right, white arrows). 40X magnification.

B) Hematoxylin and eosin (H&E) stained images of 005 GSC gliomas depicting areas of increased cell density (upper left), pseudopalisading necrosis (upper right, white arrows), and necrotic regions within the tumor (lower panels, white arrows). 40X magnification.

C) Fluorescent imaging of GFP^+ 005 GSC cells within intracranial tumors showing invasion of normal brain parenchyma by glioma cells (white arrows). 50X magnification.

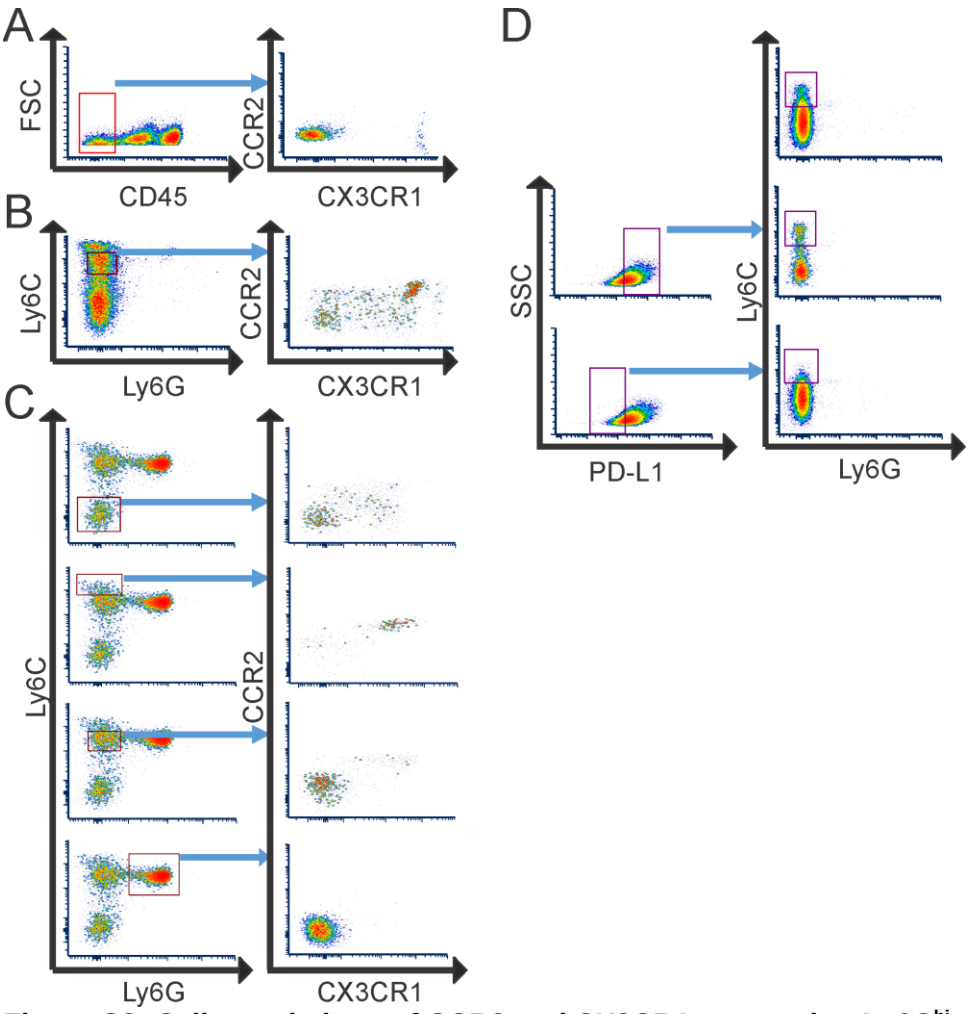

Figure S2: Cell populations of CCR2 and CX3CR1 expressing Ly6C^{hi} myeloid cells within the tumor and bone marrow of glioma bearing mice.

A) Flow cytometric analysis of tumor isolates from Ccr2$^{RFP/WT}$;Cx3cr1$^{GFP/WT}$ mice. Left panel demonstrates three distinct CD45 populations: negative (left), low (middle), and high (right). Blue arrows denote subpopulations plotted by expression of CCR2 and CX3CR1. CD45^{low} negative events represent a cell population that is CCR2^{-} and CX3CR1^{-}.

B) Flow cytometric analysis of tumor isolates from Ccr2$^{RFP/WT}$;Cx3cr1$^{GFP/WT}$ mice. Left panel represents Ly6C^{+} vs Ly6G^{+} events, and demonstrates three Ly6C populations: negative (bottom), intermediate (middle), and high (top). Blue arrows denote subpopulations plotted by expression of CCR2 and CX3CR1. Ly6C^{inter} events represent a cell population that is primarily CCR2^{+}/CX3CR1^{+}.

C) Flow cytometric analysis of bone marrow isolates from $Ccr2^{RFP/WT}$;$Cx3cr1^{GFP/WT}$ mice. Left panels represent Ly6C vs Ly6G events, and demonstrate four populations: negative (bottom), $Ly6C^{inter}/Ly6G^{-}$ (middle), $Ly6C^{hi}/Ly6G^{-}$ (top), and $Ly6C^{inter}/Ly6G^{+}$. Blue arrows denote subpopulations plotted by expression of CCR2 and CX3CR1. $Ly6C^{hi}/Ly6G^{-}$ events are primarily $CCR2^{+}/CX3CR1^{+}$. $Ly6C^{-}/Ly6G^{-}$, $Ly6C^{inter}/Ly6G^{-}$, $Ly6C^{inter}/Ly6G^{+}$ events are predominantly $CCR2^{-}/CX3CR1^{-}$.

D) Flow cytometric analysis of tumor isolates from $Ccr2^{RFP/WT}$;$Cx3cr1^{GFP/WT}$ mice. Left panel represents SSC vs $PD\text{-}L1^{+}$ events. Blue arrows denote subpopulations plotted by expression of Ly6C and Ly6G. $PD\text{-}L1^{+}$ events (upper) include $Ly6C^{hi}$ events, while $PD\text{-}L1^{-}$ events (lower) are primarily $Ly6C^{-}$ events.

Representative plots shown throughout.

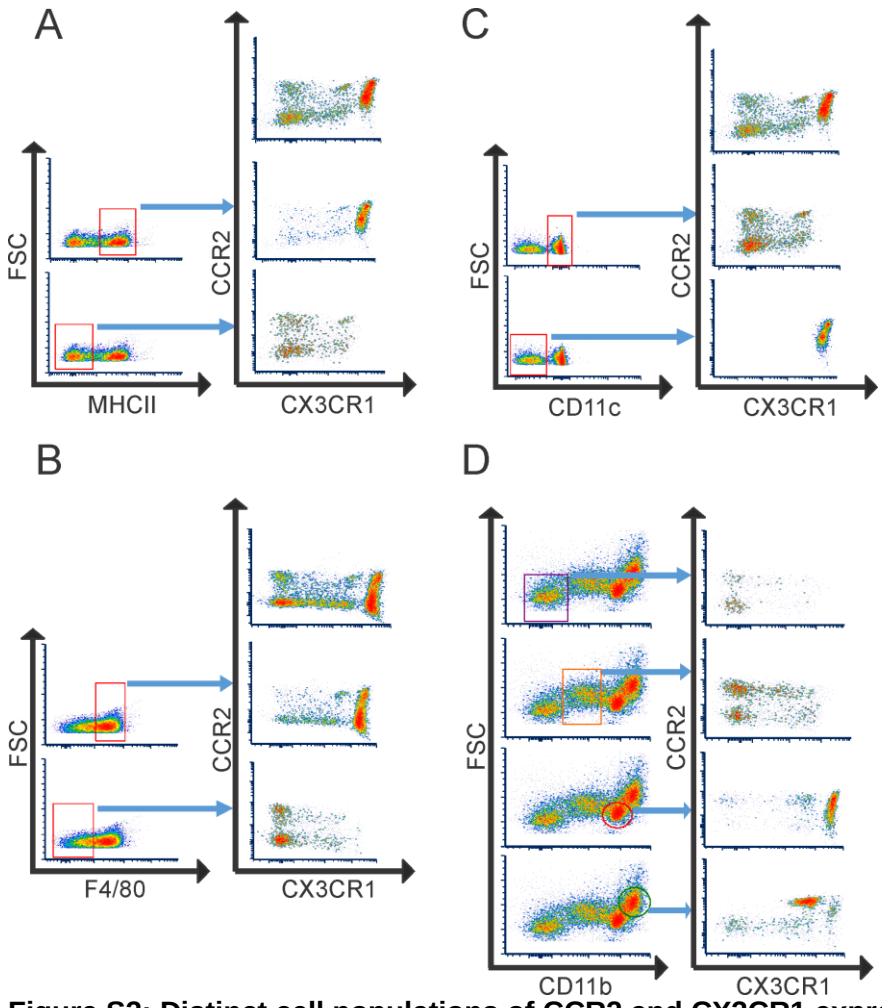

Figure S3: Distinct cell populations of CCR2 and CX3CR1 expressing myeloid cells within the tumor of glioma bearing mice.

Flow cytometric analysis of tumor isolates from $Ccr2^{RFP/WT}$;$Cx3cr1^{GFP/WT}$ mice, with left panels representing FSC vs MHCII (**A**), FSC vs F4/80 (**B**), FSC vs CD11c (**C**), or FSC vs CD11b (**D**) events. Subpopulations from each plot, negative (top) and positive (below), are shown plotted by expression of CCR2 and CX3CR1 in right panels as denoted by blue arrows. Representative plots shown throughout.

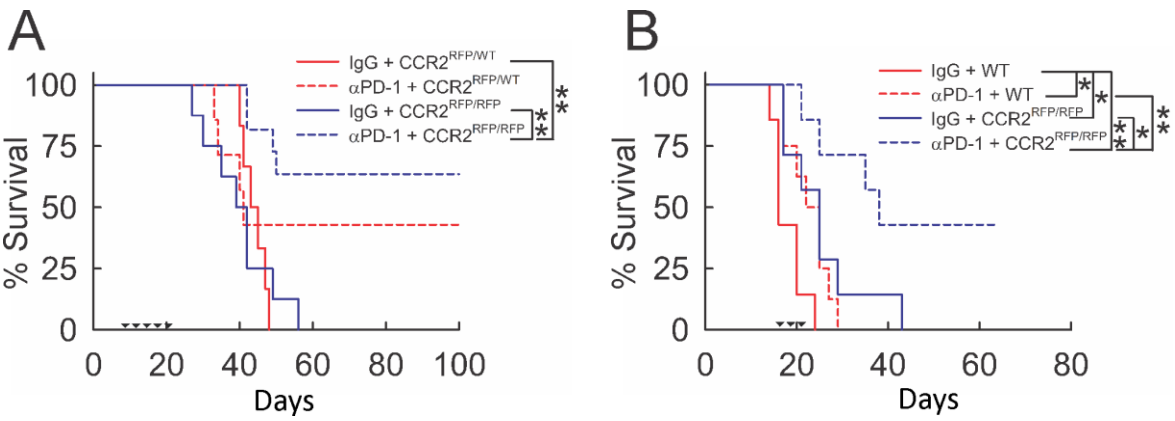

Figure S4: Impact of Ccr2 deficiency on GL261 glioma bearing mice.

A) Survival analysis of GL261 tumor bearing $Ccr2^{RFP/WT}$ and $Ccr2^{RFP/RFP}$ mice treated with or without anti-PD-1. Ccr2 deficiency (n=7) did not impact survival compared to Ccr2-sufficient ($Ccr2^{RFP/WT}$) mice (n=7). Anti-PD-1 significantly improved survival in Ccr2 deficient mice (n=7) as compared to either non-immune IgG treated $Ccr2^{RFP/WT}$ mice (p=.001) or $Ccr2^{RFP/RFP}$ animals (p=.0006). Anti-PD-1 given as a monotherapy to $Ccr2^{RFP/WT}$ mice (n=8) had no impact on median survival, but a durable survival advantage was noted. Triangles mark anti-PD-1 administration, which began at day 7, followed by 4 additional doses of anti-PD-1 given in 3 day increments (days 10, 13, 16, 19).

B) Survival analysis of GL261 tumor bearing WT and $Ccr2^{RFP/RFP}$ mice treated with or without anti-PD-1 at a later time point. Ccr2 deficiency (n=7) extended survival compared to non-immune IgG treated WT tumor bearing mice (n=7, p=.015). Monotherapy administration of anti-PD-1 (n=8) improved median survival compared to non-immune IgG treated WT mice (p=.019). Anti-PD-1 treatment of Ccr2 deficient mice (n=7) significantly enhanced survival as compared to non-immune IgG treated WT (p=.0005), anti-PD-1 monotherapy treated (p=.007), or Ccr2 deficient (p=.037) mice. A durable survival effect was only noted in anti-PD-1 treated Ccr2 deficient mice. Triangles mark anti-PD-1 administration, which began at day 14 followed by 2 additional doses of anti-PD-1 administered in 3 day increments (days 17 and 20). * = p<.05, ** = p<.01

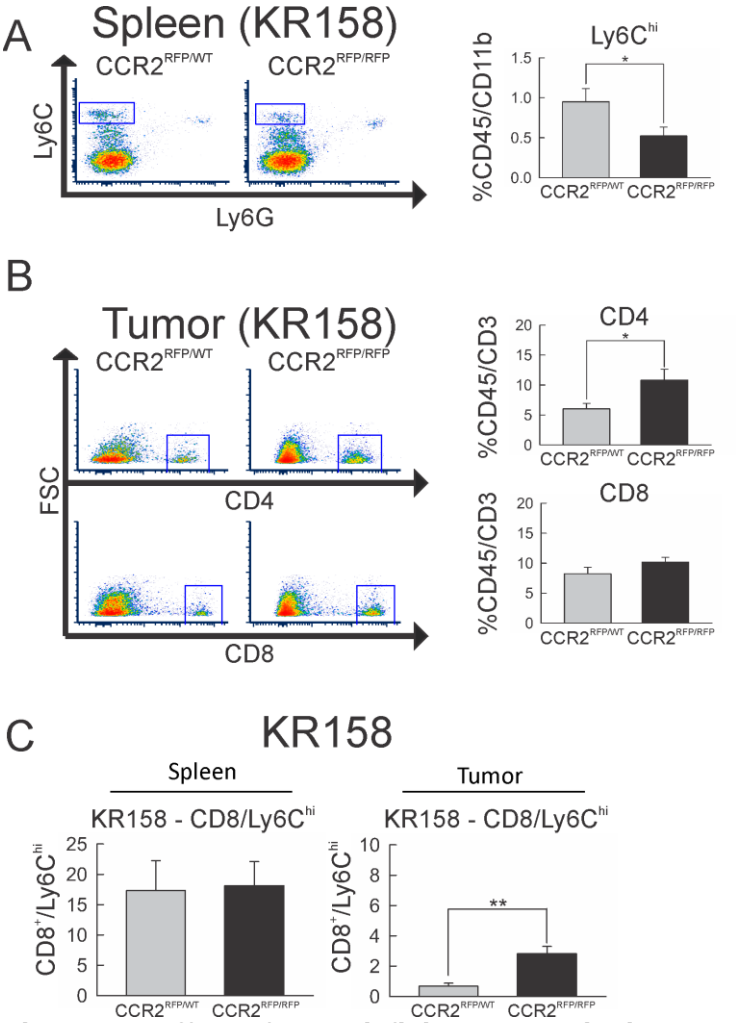

Figure S5: Effect of Ccr2 deficiency on splenic MDSC populations and tumoral T-cell populations.

A) Flow cytometric analysis of $CD45^+/CD11b^+/Ly6C^{hi}$ events. Population of $CD45^+/CD11b^+/Ly6C^{hi}$ cells within spleens were reduced (p=.048) in Ccr2 deficient animals.

B) Flow cytometric analysis of $CD45^+/CD3^+/CD4^+$ (upper) and $CD8^+$ (lower) events within tumors extracted from $Ccr2^{RFP/RFP}$ (n=10) vs. $Ccr2^{RFP/WT}$ (n=9) mice. Population of $CD45^+/CD3^+/CD4^+$ cells were increased (p=.031) in Ccr2 deficient animals. Population of $CD8^+$ cells is unchanged.

C) Quantification of the ratio of $CD45^+/CD3^+/CD8^+$ versus $CD45^+/CD11b^+/Ly6C^{hi}$ cells within the spleen (left) and tumor (right) of $Ccr2^{RFP/WT}$ (n=5) vs. $Ccr2^{RFP/RFP}$ (n=5) mice. This ratio remained

unchanged in spleen. A significant increase (p=.003) in tumors of $Ccr2^{RFP/RFP}$ vs. $Ccr2^{RFP/WT}$ mice is noted.

Representative plots shown throughout. * = p<.05, ** = p<.01

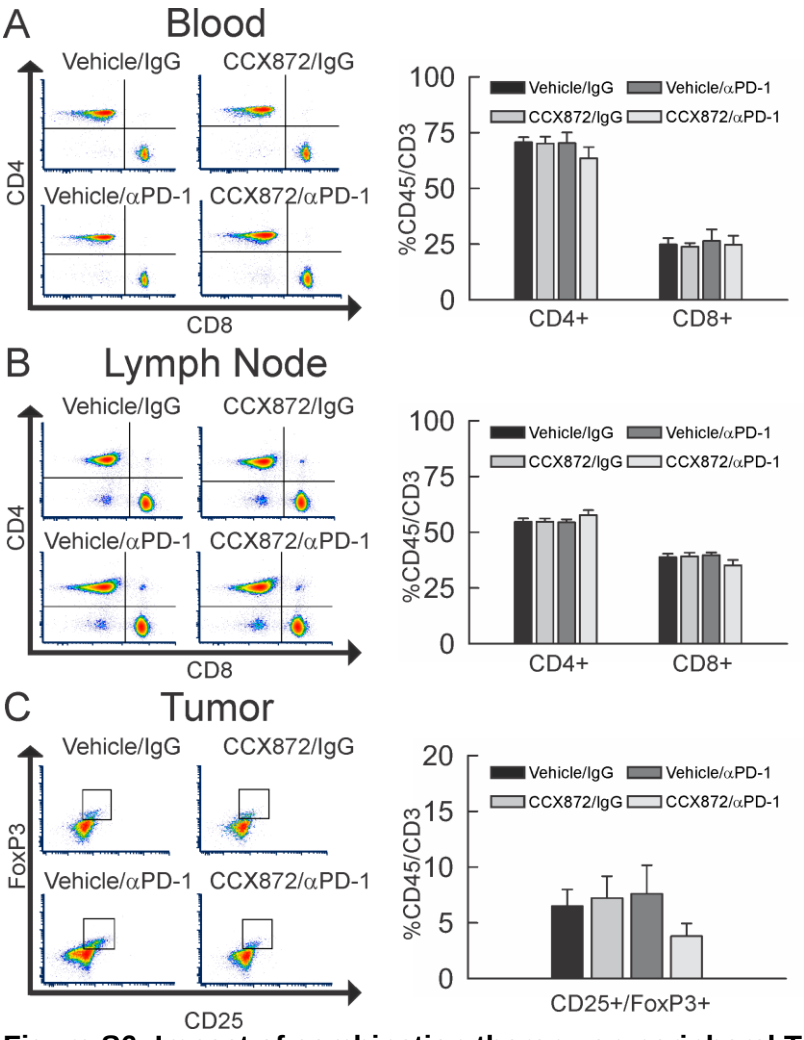

Figure S6: Impact of combination therapy on peripheral T-cell and intratumoral Treg populations.

A) Flow cytometric analysis of $CD45^+/CD3^+/CD4^+$ and $CD8^+$ events within blood extracted from Vehicle/IgG (n=5), CCX872/IgG (n=3), Vehicle/anti-PD-1 (n=4), or CCX872/anti-PD-1 (n=3) treated 005 GSC glioma bearing mice. Population of $CD45^+/CD3^+/CD4^+$ cells remained unchanged in all treatment groups. Representative plots shown throughout.

B) Flow cytometric analysis of $CD45^+/CD3^+/CD4^+$ and $CD8^+$ events within draining lymph nodes extracted from Vehicle/IgG (n=6), CCX872/IgG (n=3), Vehicle/anti-PD-1 (n=5), or CCX872/anti-PD-1 (n=3) treated 005 GSC glioma bearing mice. Population of $CD45^+/CD3^+/CD4^+$ cells remained unchanged in all treatment groups.

C) Flow cytometric analysis of $CD45^+/CD3^+/FoxP3^+/CD25^+$ events within tumors from Vehicle/IgG (n=5), CCX872/IgG (n=3), Vehicle/anti-PD-1 (n=4), or CCX872/anti-PD-1 (n=5) treated 005 GSC glioma bearing mice. Population of $CD45^+/CD3^+/FoxP3^+/CD25^+$ cells remained statistically unchanged in all treatment groups, with a trend (p=.19) toward decrease in combination therapy treated animals.

Representative plots shown throughout.

Supplement Table 1:

Flow Cytometry

Protein	Fluorophore	Company	Catalog #	Dilution Factor
CD11b	APC/Cy7	Biolegend	101226	1:100
Ly6G	APC	Biolegend	127613	1:100
Ly6C	FITC	Biolegend	128005	1:100
CD3	APC/Fire750	Biolegend	100362	1:100
CD8a	APC	Biolegend	100712	1:100
CD4	APC	Biolegend	100516	1:100
CD45	Alexa700	Biolegend	103128	1:200
CD11b	BV421	Biolegend	101251	1:100
Ly6G	PerCP	Biolegend	127654	1:100
Ly6C	BV785	Biolegend	128041	1:100
CD4	FITC	Biolegend	100510	1:100
CD3	BV510	Biolegend	100234	1:100
Tim3	BV421	Biolegend	119723	1:100
PD-1	PE	BD Pharmigen	551892	1:100
MHCII	BV510	Biolegend	107636	1:100
F4/80	APC	Biolegend	123116	1:100
CD11c	FITC	Biolegend	117306	1:100
FoxP3	PE-Cy7	Invitrogen	25-5773-82	1:50
CD25	PE	Biolegend	101904	1:100
PD-L1	APC	Biolegend	124312	1:100
Live/Dead	Pacific Blue	Invitrogen	L34963	1μl/ml

Biolegend, San Diego CA; BD Pharmigen, San Jose CA; Invitrogen, Carlsbad, CA

IHC: rat anti-CD11b (dilution 1:50, Biolegend, San Diego CA).